Original Research

Application of Polynomial Regression Model for Joint Stiffness

YOUNGMIN CHUN[†1], CRAIG P. MCGOWAN[‡2], JINAH KIM[‡3], and JOSHUA P. BAILEY[‡4]

[1]Department of Kinesiology, Sonoma State University, Rohnert Park, CA, USA, [2]Department of Integrative Anatomical Sciences, University of Southern California, Los Angeles, CA, USA, [3]Department of Physical Education, Yonsei University, Seoul, South Korea, [4]Department of Movement Sciences, University of Idaho, Moscow, ID, USA

[†]Denotes graduate student author, [‡]Denotes professional author

ABSTRACT

International Journal of Exercise Science 15(1): 1236-1245, 2022. Quasi-stiffness (joint stiffness) is often used to characterize leg properties during athletic and other activities and has been reported by a single slope of angle-moment curve. However, the joint angle-moment relationship of some relationship are not effectively represented by a simple linear regression model. Thus, the purpose of this analysis was to investigate the benefits of utilizing a 2nd order polynomial regression (quadratic) model as compared to the linear model when calculating lower extremity joint stiffness incorporating subdivided eccentric phases. Thirty healthy and active college students performed 15 drop jumps from a 30-cm platform. The eccentric phase was identified as the time from initial foot contact (IC) to the lowest vertical position of the center of mass and subdivided into the loading and attenuation phases, separated by the peak vertical ground reaction force. Lower extremity joint stiffnesses (hip, knee, and ankle) for the loading and attenuation phases were calculated using a linear and quadratic model. Multiple 2 by 2 repeated measures ANOVAs were performed. In the post-hoc analyses, the quadratic model had greater goodness-of-fit (r^2 and RMSE) than the linear model ($p < .05$) for all joints. The quadratic model revealed differences between the loading and attenuation phases for both hip ($p = .001$) and knee stiffness ($p < .001$). These results suggest that the quadratic model is more representative of the angle-moment relationship while subdividing the eccentric phase of a drop jump into the loading and attenuation phases.

KEY WORDS: Quadratic model, angle-moment relationship, landing mechanics

INTRODUCTION

In physics, the notion of stiffness has been used to describe properties of deformable objects in response to the external load(15). This notion was also applied to biomechanics research by introducing the spring-mass system to the human body (4). Specifically, lower extremity stiffness has been utilized to measure the related load and displacement characteristics in sport-related activities to evaluate performance (2, 22) and identify potential injury risk (8, 19, 21). Stiffness of the lower extremity can be reported as leg stiffness, representing the lower extremity as a spring (2, 4, 17, 19), or by investigating the quasi-stiffness of each joint independently,

considering each joint as a torsional spring (2, 8, 15, 21, 22). Leg stiffness reflects the ability of all the lower extremity structures to resist the vertical displacement of the center of mass (COM) with respect to the vertical ground reaction force (vGRF) (2, 17, 19) whereas quasi-stiffness (joint stiffness) identifies joint-specific responses to loads (6, 8, 15, 21).

A commonly used mathematical model to estimate joint stiffness is a linear regression (linear) model using the angle-moment relationship (2, 8, 21, 22). This linear model has commonly been used to calculate joint stiffness and reported high coefficients of determination (r^2) (8, 21, 22). However, in many cases, the simple linear model likely does not accurately represent the joint angle-moment relationship as the direction of the changes in the joint angle and moment could be different from each other. This is demonstrated through hip stiffness during a drop jump, as the external hip flexion moment may decrease at the beginning of the landing phase and then increase until the end of the landing phase. This moment is coupled with a sagittal hip angle continuously increasing the flexion angle during the phase (8, 21), which causes a curvilinear relationship between joint angle and moment. The line of best fit obtained by the linear model does not accurately represent this curvilinear relationship. The error in the stiffness model may be magnified as the contact time decreases (2).

Moreover, calculating joint stiffness as a single value may also overlook time-varying changes in the angle-moment relationship. For example, a linear model has been utilized to calculate joint stiffness for the entire ground contact period or the eccentric phase during running (22) or drop jumps (8). However, the mechanical property of the joint may be over- or underestimated by a single value of joint stiffness in that each joint's contribution to absorb the kinetic energy during subdivided eccentric phases may differ (10). Thus, calculating joint stiffness for subdivided eccentric phases would provide a better understanding of changes in the mechanical property of joints.

Thus, the purpose of this analysis was to investigate the benefits of a 2nd order polynomial regression (quadratic) model to calculate joint stiffness for subdivided eccentric phases as compared to a linear model. We hypothesized that the quadratic model would more accurately indicate best-fit lines in angle-moment relationships than a linear model and would more accurately detect changes in joint stiffness by the tangent slopes.

METHODS

Participants
Thirty healthy and active college students were recruited (Males: Height = 1.82 ± 0.04 m, Mass = 82.4 ± 12.1 kg, Age = 25.8 ± 6.6 years; Females: Height = 1.71 ± 0.09 m, Mass = 64.5 ± 11.2 kg, Age = 25.2 ± 9.2 years) by a convenience sampling. All participants in this study were considered physically active and healthy individuals who are regularly engaged in physical activities at least 30 minutes with moderate-intensity for 5 days per week or at least 20 minutes with vigorous-intensity for 3 days per week (11). Also, they were free from lower extremity injuries within the past year and had no history of surgery to the lower extremity, pelvis, and low back.

The data for this analysis were taken from a larger study protocol that was approved by the university institutional review board and all participants gave written consent before participation. This research was carried out fully in accordance to the ethical standards of the International Journal of Exercise Science (18).

Protocol
A limb for the analysis was conveniently selected by identifying a preferred limb to kick a ball (7) as this study was not focused on bilateral limb differences. Participants performed a self-selected warm-up for at least 5 minutes, and then a customized full-body marker set was applied to bony landmarks for each segment. Four clusters were used to track thigh and shank segments.

Participants performed drop vertical jumps from a 30-cm platform to minimize the effect of drop jump height on the ground contact time (1). The platform was positioned at the distance equal to half of the participant's height away from two embedded force platforms. To perform the drop jump, participants were instructed to stand on the edge of the platform and drop off without jumping up while landing with one foot on each force platform (20). They were then instructed to perform a maximal vertical jump immediately upon contacting the ground. Two practice trials were given and then 15 good trials (i.e., both feet on the center of platforms) were collected.

The drop vertical jump trials were captured using a 3-D motion capture system with 8 infrared cameras (VANTAGE 5, Vicon Motion System Ltd., Oxford, UK) and two embedded force platforms (OR6-6, AMTI, Watertown, MA, USA). The motion capture and ground reaction force (GRF) data were collected at 250 Hz and 1000 Hz, respectively. A power spectral density analysis was performed to determine the cut-off frequency for filtering using data from the lower extremity markers and a customized MATLAB script (MATLAB 2019b, MathWorks, Natick, MA, USA). An optimal cut-off frequency was determined to be the frequency that retained 99% of the marker trajectory signals. Both marker trajectory and GRF data were lowpass filtered at the optimal cut-off frequency of 11 Hz, using a 2nd order Butterworth filter (13). The filtered data were transported to Visual3D (Visual3D v6 Professional, C-Motion, Inc., Germantown, MA, USA) to calculate lower extremity joint angles, external moments, and COM of the complete skeletal model. The joint angles were calculated using a Cardan (XYZ) rotation sequence. The external joint moments were resolved in the distal segment coordinate system and normalized to body mass ($N \cdot m \cdot kg^{-1}$). The direction of rotation of lower extremity joint angles and external moments were matched, with positive values indicating hip flexion, knee flexion, and ankle dorsiflexion rather than following the right-hand rule.

Initial foot contact (IC) was identified using a vGRF threshold of 20 N (13, 14). The eccentric phase was identified as the time from IC to the time at the lowest vertical position of the COM. The eccentric phase was then subdivided into the loading (i.e., IC to peak vGRF) and attenuation phases (i.e., peak vGRF to the lowest vertical position of the COM) using the temporal location of peak vGRF (9, 10). The subdivided landing phases were operationally defined by the reaction of the body to the external load. The loading phase represents a short period of time in which

the body passively resists the impact force, and the attenuation phase indicates a period of time to actively attenuate the external load by the active structures. The joint angles and moments for 15 trials were interpolated to 101 data points and then averaged. The best-fit line of joint angle-moment relationships were calculated using a linear model (8, 19, 21) and a quadratic model during each phase (Equation 1).

$$Equation\ 1: \hat{y}_i = \beta_0 x_i^2 + \beta_1 x_i + \beta_2$$

Where $\hat{y}_i$ is the estimated joint moment at ith frame for the best-fit curve, x_i is the joint angle at ith frame, and the β_0 is the coefficient of x^2 that represents the width and convexity (or concavity) of the curve (Figure 1). The vertex position of the curve (angle = h, moment = k), can be determined by combinations of coefficients (Equation 2) based on the vertex form of Equation 1 (Figure 1).
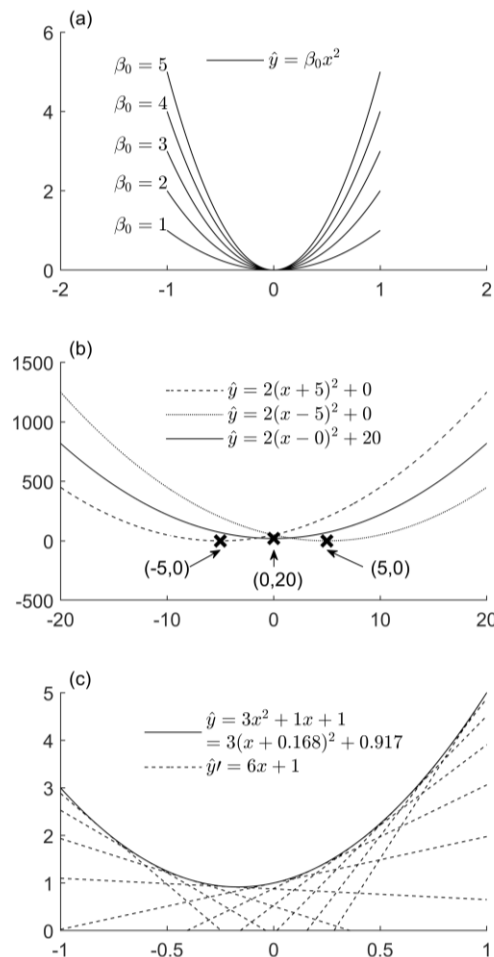

Figure 1. Determination of the best-fit line shapes by coefficients of the quadratic model. (a) The coefficient of x^2 determines concavity (or convexity) and width of the best-fit line. (b) The vertex form of the model indicates the location of the vertex of the best-fit line. (c) The differentiated best-fit line indicates the slope of tangent lines for each data point.

$$Equation\ 2.1: \hat{y}_i = \beta_0 (x_i - h)^2 + k$$

$$Equation\ 2.2: h = \frac{\beta_1}{2\beta_0}$$

$$Equation\ 2.3: k = \beta_2 - \beta_0 h^2$$

Since the quadratic does not directly provide a slope of the curve, the function was differentiated to obtain the slope of the tangent lines (Equation 3).

$$Equation\ 3: \hat{y}_i' = 2\beta_0 x + \beta_1$$

Using Equation 3, tangent slopes of all data points of the best-fit curve represent the instantaneous joint stiffness. The slopes are then averaged throughout the loading and attenuation phases, respectively, to represent the joint stiffness. The obtained stiffness is then compared with the stiffness calculated by the linear model (Figure 1). The root mean squared error (RMSE) and r^2 were calculated using Equation 4 to both relatively and absolutely evaluate the best-fit lines of two models (2,8,19). r^2 indicates how well the best-fit line represents the angle-moment relationship using the scale from 0 to 1 whereas RMSE represents the average distance between the observed data and the best-fit line.

$$Equation\ 4.1: r^2 = 1 - \frac{\sum_{i=1}^{n}(y_i - \hat{y}_i)^2}{\sum_{i=1}^{n}(y_i - \bar{y})^2}$$

$$Equation\ 4.2: RMSE = \sqrt{\frac{\sum_{i=1}^{n}(y_i - \hat{y}_i)^2}{n}}$$

Where $\bar{y}$ is the average joint moment during each phase.

Statistical Analysis
The Shapiro-Wilk tests and Levene's tests were performed to assess the normal distribution of data and the homogeneity of variance assumption. Multiple 2 by 2 repeated measures ANOVAs were performed using R (23). The independent variables were model (quadratic vs. linear) and phase (loading vs. attenuation). The dependent variables were hip, knee, and ankle stiffness, r^2, and RMSE. The a priori α level was set at .05. If a significant interaction effect was found, a *post-hoc* pairwise-comparison was performed with *Bonferroni p*-value adjustment ($p = 0.008$). The *post-hoc* analyses were reported only for the comparisons of interest between phases in the same model and between models in the same phase. This is because it is not meaningful to compare the values across models and phases in this study. Partial ω^2 (ω^2) was reported to indicate the magnitude of difference (small = 0.01, medium = 0.06, large = 0.14) (12).

RESULTS

The normal distribution and homogeneity of variance for all dependent variables were identified ($p > .05$). Significant interactions between model and phase were observed in r^2 of all joints (Hip: $F(1,29) = 31.956$, $p < .001$, $\omega^2 = 0.175$; Knee: $F(1,29) = 14.593$, $p < .001$, $\omega^2 = 0.076$;

Ankle: $F(1,29) = 11.084$, $p = .002$, $\omega^2 = 0.059$) and RMSE of hip ($F(1,29) = 6.253$, $p = .018$, $\omega^2 = 0.016$) and ankle joint stiffness ($F(1,29) = 11.499$, $p = 0.002$, $\omega^2 = 0.073$). Significant model main effects in r^2 (Hip: $F(1,29) = 72.406$, $p < .001$, $\omega^2 = 0.362$; Knee: $F(1,29) = 28.986$, $p < .001$, $\omega^2 = 0.135$; Ankle: $F(1,29) = 26.761$, $p < .001$, $\omega^2 = 0.126$) and RMSE (Hip: $F(1,29) = 145.043$, $p < .001$, $\omega^2 = 0.269$; Knee: $F(1,29) = 55.958$, $p < .001$, $\omega^2 = 0.325$; Ankle: $F(1,29) = 93.255$, $p < .001$, $\omega^2 = 0.421$) in all joints were observed. Significant phase main effects in r^2 of knee stiffness ($F(1,29) = 37.401$, $p < .001$, $\omega^2 = 0.383$) and RMSE of knee ($F(1,29) = 5.364$, $p = .028$, $\omega^2 = 0.080$) and ankle stiffness ($F(1,29) = 9.745$, $p = .004$, $\omega^2 = 0.152$) were found (Table 1).

Significant interactions between model and phase were found in stiffness of all joints (Hip: $F(1,29) = 19.574$, $p < .001$, $\omega^2 = 0.015$; Knee: $F(1,29) = 5.223$, $p = .030$, $\omega^2 = 0.003$; Ankle: $F(1,29) = 4.967$, $p = .034$, $\omega^2 = 0.001$). Significant model main effects in knee ($F(1,29) = 38.550$, $p < .001$, $\omega^2 = 0.030$) and ankle stiffness ($F(1,29) = 18.827$, $p < .001$, $\omega^2 = 0.004$) and significant phase main effects in hip ($F(1,29) = 7.439$, $p = .011$, $\omega^2 = 0.082$) and knee stiffness ($F(1,29) = 112.889$, $p < .001$, $\omega^2 = 0.660$) were observed (Table 1).

Table 1. Coefficient of determination (r^2) and stiffness calculated by each model.

	Loading		Attenuation	
	Linear	Quadratic	Linear	Quadratic
Stiffness ($N \cdot m \cdot kg^{-1} \cdot °^{-1}$)				
Hip[†,‡]	0.022 ± 0.044[‖]	0.101 ± 0.052[#]	0.044 ± 0.050	0.052 ± 0.058
Knee[*,†,‡]	0.052 ± 0.014[§,‖]	0.049 ± 0.015[#]	0.009 ± 0.017[¶]	0.004 ± 0.017
Ankle[*,‡]	0.027 ± 0.023	0.029 ± 0.017	0.046 ± 0.090[¶]	0.057 ± 0.099
RMSE ($N \cdot m \cdot kg^{-1} \cdot °^{-1}$)				
Hip[*,‡]	0.114 ± 0.044[‖]	0.047 ± 0.024	0.124 ± 0.089[¶]	0.082 ± 0.074
Knee[*,†]	0.071 ± 0.030	0.033 ± 0.012	0.094 ± 0.053	0.058 ± 0.050
Ankle[*,†,‡]	0.030 ± 0.022[§,‖]	0.015 ± 0.020	0.055 ± 0.024[¶]	0.024 ± 0.015
r^2				
Hip[*,‡]	0.561 ± 0.310[§,‖]	0.925 ± 0.067	0.782 ± 0.225[¶]	0.872 ± 0.188
Knee[*,†,‡]	0.966 ± 0.049[§,‖]	0.994 ± 0.004[#]	0.587 ± 0.311[¶]	0.785 ± 0.254
Ankle[*,‡]	0.903 ± 0.235[‖]	0.934 ± 0.189	0.755 ± 0.263[¶]	0.922 ± 0.110

Note: [*]Significant model main effect ($p < .05$). [†]Significant phase main effect ($p < .05$). [‡]Significant interaction effect between model and phase ($p < .05$). [§]Significant *post-hoc* analysis between the loading phase of the linear model and the attenuation phase of the linear model ($p < .05$). [‖]Significant *post-hoc* analysis between the loading phase of the linear model and the loading phase of the quadratic model ($p < .05$). [¶]Significant *post-hoc* analysis between the attenuation phase of the linear model and the attenuation phase of the quadratic model ($p < .05$).
[#]Significant *post-hoc* analysis between the loading phase of the quadratic model and the attenuation phase of the quadratic model ($p < .05$).

DISCUSSION

This study was aimed at identifying benefits of a quadratic model to calculate lower extremity joint stiffness in subdivided eccentric phases. The results of the present analyses support our hypothesis that the quadratic model provides better best-fit lines in joint angle-moment relationships. Our major findings were the quadratic model indicated greater *r^2* and lower

RMSE for all joint angle-moment relationships than linear model. Differences in hip and knee stiffness were identified using the quadratic model when compared to the linear model.
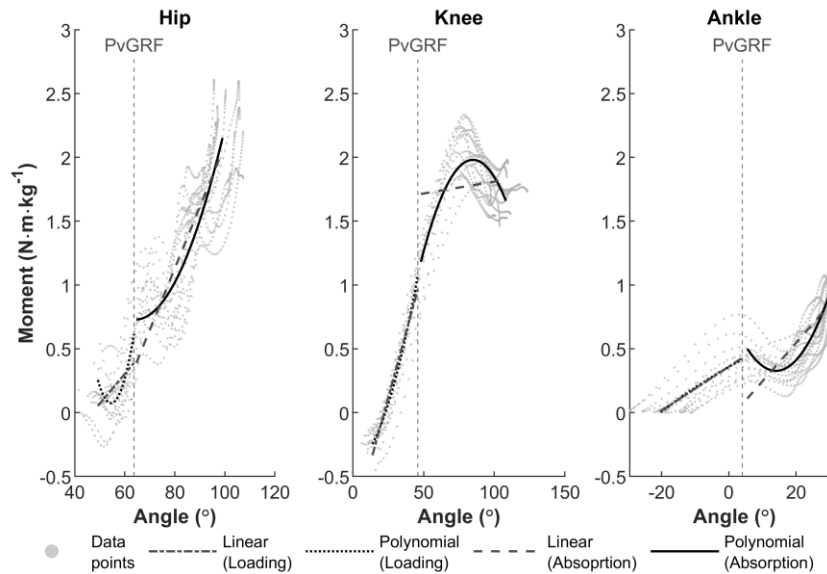

Figure 2. Angle-moment curves with the best-fit line estimated by both linear and quadratic models for each loading and attenuation phase using 15 trials of drop jump of a single participant.

Hip (Linear model during loading phase: $\hat{y} = 0.023x - 1.10$, $r^2 = 0.442$; Polynomial model during loading phase: $\hat{y} = 0.007x^2 - 0.706x + 19.311$, $r^2 = 0.967$; Linear model during attenuation phase: $\hat{y} = 0.048x - 2.731$, $r^2 = 0.924$; Polynomial model during attenuation phase: $\hat{y} = 0.001x^2 - 0.151x + 5.572$, $r^2 = 0.972$);

Knee (Linear model during loading phase: $\hat{y} = 0.041x - 0.892$, $r^2 = 0.981$; Polynomial model during loading phase: $\hat{y} = 0.001x^2 + 0.005x - 0.425$, $r^2 = 0.998$; Linear model during attenuation phase: $\hat{y} = 0.002x + 1.624$, $r^2 = 0.032$; Polynomial model during attenuation phase: $\hat{y} = -0.001x^2 + 0.1x - 2.263$, $r^2 = 0.899$);

Ankle (Linear model during loading phase: $\hat{y} = 0.017x + 0.360$, $r^2 = 0.996$; Polynomial model during loading phase: $\hat{y} = -0.0001x^2 + 0.015x + 0.35$, $r^2 = 0.998$; Linear model during attenuation phase: $\hat{y} = 0.030x - 0.055$, $r^2 = 0.771$; Polynomial model during attenuation phase: $\hat{y} = 0.002x^2 - 0.067x + 0.795$, $r^2 = 0.988$).

The quadratic model more accurately represented the joint angle-moment relationships for all joints and phases, compared to the linear model. The linear model represented fairly good lines of best-fit for the joint angle-moment curves in the distal joints (knee and ankle) during the loading phase (Table 1 and Figure 2), but the linear model failed to represent the angle-moment relationship during the attenuation phase. It is likely that the linear model was able to represent the angle-moment relationship only during the loading phase because the muscle-tendon unit of the lower extremities are fully engaged during the attenuation phase in response to the external load due to electromechanical delays (5) and laxity of structures. Our data indicated the average time to reach peak VGRF was approximately 50 ms like observed in previous studies (3, 9, 10), similar to the electromechanical delays of muscle (5). Thus, the muscle activation combined with the gravitational force might gradually increase the force production with the increasing joint angles up to the peak vGRF appearance, and then regulate external load for each joint during the attenuation phase. However, following the loading phase, the muscle-tendon units actively resist the external load and cause changes in the joint moment throughout the attenuation phase.
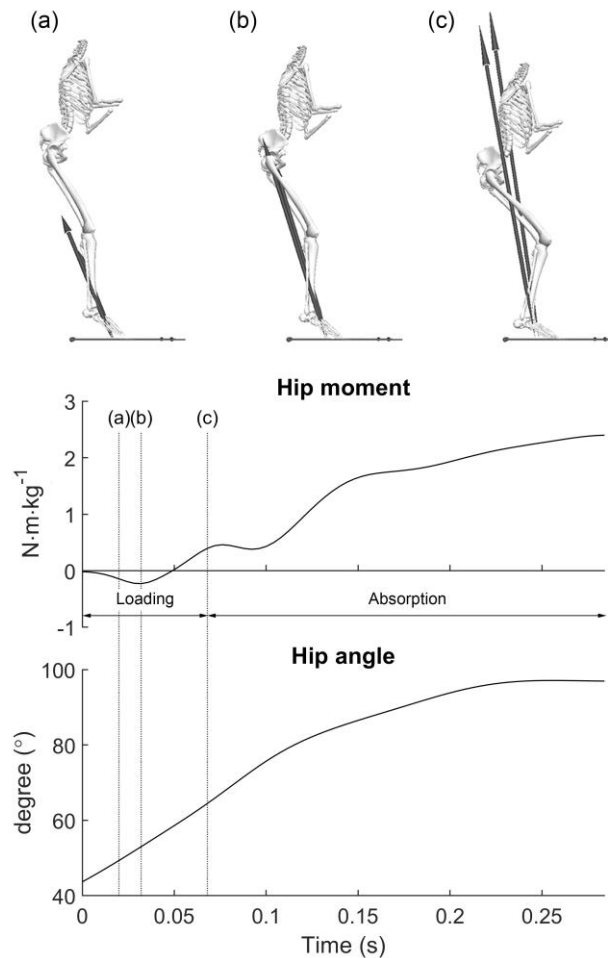
Figure 3. The changes in the hip joint angle and moment by the direction of the resultant GRF vector during the eccentric phase of the drop jump. (a) 20 ms after IC, (b) minimum hip joint moment, and (c) the end of the loading phase (i.e., at peak vertical ground reaction force).

Additionally, the hip joint had a curvilinear relationship between joint angle and moment even in the loading phase as opposed to the distal joints. Based on the observations in this study, the curvilinear relationship during the loading phase seems to be attributed to the changes in the direction of the resultant GRF vector, which mostly affected the moment of the hip. As seen in Figure 3, the external hip moment kept decreasing after IC until the resultant GRF vector passed the hip joint center, and then increased during the rest of the loading phase. This created a curvilinear relationship between the hip angle and moment, which suggested that the quadratic model could indicate better representation (22). Indeed, the subdivided phases illustrated the benefit of the polynomial equation was greater during the attenuation phase across all lower extremity joints.

The quadratic model indicated changes in joint stiffness at the hip and knee between the loading and attenuation phase whereas the linear model detected the difference only at knee. The joint stiffness obtained by the quadratic model is likely more sensitive to the joint angle-moment

relationship than the linear. For instance, the linear model omits the negative relationship between joint angle and moment as seen in Figure 2, but the quadratic model encompasses the negative slope in the average. The omitted curvilinear or negative relationship caused by the linear model could over- or underestimate the joint stiffness. The linear model likely underestimated the hip joint stiffness during the loading phase ($0.022 \pm 0.044 \; N \cdot m \cdot kg^{-1} \cdot °^{-1}$) due to the offset induced by the poor best-fit line as compared to the stiffness ($0.101 \pm 0.052 \; N \cdot m \cdot kg^{-1} \cdot °^{-1}$) calculated by the quadratic model (Table 1 and Figure 2). Also, the average slope (i.e., joint stiffness derived from the quadratic model) of the best-fit line relies on the position of the best-fit line vertex. If the vertex of the fitted line with convex shape is positioned at the early or even before the phase, the averaged slope is most likely to be close to zero or even indicate negative joint stiffness (e.g., knee stiffness during the attenuation phase; Table 1 and Figure 2).

The present study has a couple of potential limitations. The fixed height of drop jump platform (30 cm), rather than a percentage of participants height or leg length, was provided for all participants. This potentially affects joint stiffness in that each individual could have different perceived intensity of the external load in relation to their functional capacity to resist the external loads. Another limitation of this study is that the shoes were not controlled. All participants were allowed to wear their own athletic shoes that have different mechanical properties across participants' shoes. The different shoes could affect the interaction between the performer and the ground, specifically the vGRF (16), which could cause differences between the participants' joint stiffness responses.

In summary, details about changes in joint stiffness were obtained by the quadratic model with subdivided eccentric phases, and this model provided better fitted line to obtain joint stiffness as compared to the linear model. The use of the quadratic model for subdivided eccentric phases would provide insight of changes in joint stiffness to absorb and transmit the external loads for the subsequent task.

ACKNOWLEDGEMENTS

REFERENCES

1. Addie CD, Arnett JE, Neltner TJ, Straughn MK, Greska EK, Cosio-Lima L, et al. Effects of drop height on drop jump performance. Int J Kinesiol Sport Sci 7(4): 28-32, 2019.

2. Arampatzis A, Schade F, Walsh M, Brüggemann G-P. Influence of leg stiffness and its effect on myodynamic jumping performance. J Electromyogr Kinesiol 11(5): 355–64, 2001.

3. Bates NA, Ford KR, Myer GD, Hewett TE. Impact differences in ground reaction force and center of mass between the first and second landing phases of a drop vertical jump and their implications for injury risk assessment. J Biomech 46(7): 1237–41, 2013.

4. Blickhan R. The spring-mass model for running and hopping. J Biomech 22(11–12): 1217–27, 1989.

5.   Cavanagh PR, Komi PV. Electromechanical delay in human skeletal muscle under concentric and eccentric contractions. Eur J Appl Physiol Occup Physiol 42(3): 159–63, 1979.

6.   Farley CT, Morgenroth DC. Leg stiffness primarily depends on ankle stiffness during human hopping. J Biomech 32(3): 267–73, 1999.

7.   Ford KR, Myer GD, Hewett TE. Valgus knee motion during landing in high school female and male basketball players. Med Sci Sports Exerc 35(10): 1745–50, 2003.

8.   Ford KR, Myer GD, Hewett TE. Longitudinal effects of maturation on lower extremity joint stiffness in adolescent athletes. Am J Sports Med 38(9): 1829–37, 2010.

9.   Harry JR, Barker LA, Eggleston JD, Dufek JS. Evaluating performance during maximum effort vertical jump landings. J Appl Biomech 34(5): 403–9, 2018.

10.   Harry JR, Barker LA, James R, Dufek JS. Performance differences among skilled soccer players of different playing positions during vertical jumping and landing. J Strength Cond Res 32(2): 304–12, 2018.

11.   Haskell WL, Lee IM, Pate RR, Powell KE, Blair SN, Franklin BA, et al. Physical activity and public health: Updated recommendation for adults from the American College of Sports Medicine and the American Heart Association. Med Sci Sports Exerc 39(8): 1423–34, 2007.

12.   Kotrlik J, Williams H, Jabor K. Reporting and interpreting effect size in quantitative agricultural education research. J Agric Educ 52(1): 132–42, 2011.

13.   Kristianslund E, Krosshaug T, Van den Bogert AJ. Effect of low pass filtering on joint moments from inverse dynamics: Implications for injury prevention. J Biomech 45(4): 666–71, 2012.

14.   Krosshaug T, Steffen K, Kristianslund E, Nilstad A, Mok K-M, Myklebust G, et al. The vertical drop jump is a poor screening test for acl injuries in female elite soccer and handball players: A prospective cohort study of 710 athletes. Am J Sports Med 44(4): 874–83, 2016.

15.   Latash ML, Zatsiorsky VM. Joint stiffness: Myth or reality? Hum Mov Sci 12(6): 653–92, 1993.

16.   Logan S, Hunter I, J Ty Hopkins JT, Feland JB, Parcell AC. Ground reaction force differences between running shoes, racing flats, and distance spikes in runners. J Sports Sci Med 9(1): 147–53, 2010.

17.   Morin J-B, Dalleau G, Kyröläinen H, Jeannin T, Belli A. A simple method for measuring stiffness during running. J Appl Biomech 21(2): 167–80, 2005.

18.   Navalta JW, Stone WJ, Lyons TS. Ethical issues relating to scientific discovery in exercise science. Int J Exerc Sci 12(1): 1–8, 2019.

19.   Padua DA, Garcia CR, Arnold BL, Granata KP. Gender differences in leg stiffness and stiffness recruitment strategy during two-legged hopping. J Mot Behav 37(2): 111–25, 2005.

20.   Padua DA, Marshall SW, Boling MC, Thigpen CA, Garrett WE, Beutler AI. The landing error scoring system (less) is a valid and reliable clinical assessment tool of jump-landing biomechanics the jump-acl study. Am J Sports Med 37(10): 1996–2002, 2009.

21.   Schmitz RJ, Shultz SJ. Contribution of knee flexor and extensor strength on sex-specific energy absorption and torsional joint stiffness during drop jumping. J Athl Train 45(5): 445–52, 2010.

22.   Stefanyshyn DJ, Nigg BM. Dynamic angular stiffness of the ankle joint during running and sprinting. J Appl Biomech 14(3): 292–9, 1998.

23.   Team RC. R: A language and environment for statistical computing. Vienna, Austria: R Foundation for Statistical Computing; 2020.